Toward the Ultimate RTK: The Last Challenges in Long-Range Real-Time Kinematic Applications

Don Kim and Richard B. Langley

Geodetic Research Laboratory, Department of Geodesy and Geomatics Engineering
University of New Brunswick, Fredericton, New Brunswick, Canada

BIOGRAPHIES

Don Kim is a senior research associate and a faculty member in the Department of Geodesy and Geomatics Engineering at the University of New Brunswick (UNB). He has a bachelor's degree in urban engineering, and an M.Sc.E. and Ph.D. in geomatics from Seoul National University. He has been involved in GPS research since 1991 and active in the development of an ultrahigh-performance RTK system for the past few years. He received the Dr. Samuel M. Burka Award for 2003 from The Institute of Navigation (ION). He also shared two IEEE/ION PLANS Best Track Paper Awards for 2006 and 2008.

Richard B. Langley is a professor in the Department of Geodesy and Geomatics Engineering at UNB, where he has been teaching since 1981. He has a B.Sc. in applied physics from the University of Waterloo and a Ph.D. in experimental space science from York University, Toronto. Prof. Langley has been active in the development of GPS error models since the early 1980s and is a contributing editor and columnist for GPS World magazine. He is a fellow of the ION and the Royal Institute of Navigation and shared the ION 2003 Burka Award with Don Kim, and received the ION's Kepler Award in 2007.

ABSTRACT

Although significant improvements in handling the unmodelled atmospheric (i.e., ionospheric and tropospheric) delays for long-range RTK (real-time kinematic) applications have been made by many research groups over the world, it is often found that the residual tropospheric delay is still the most problematic error source for such applications. One of the most challenging issues with respect to the residual tropospheric delay is that the two coefficients associated with the tropospheric zenith delay and the up component of a positioning solution (i.e., the tropospheric mapping functions and the up components of the design matrix) are almost linearly correlated above a 20 degree elevation angle. In this case, variations in the tropospheric zenith delay are almost indistinguishable from those in the up component at high elevation angles. In the conventional approaches, satellites being observed at low elevation angles can help the least-squares estimator break up the correlation associated with two parameters. If no satellite is available at low elevation angles, an adaptive estimator of the tropospheric zenith delay can relieve the problem to some degree.

In this paper, we propose a new approach to overcome the challenges associated with the residual tropospheric delay. The tropospheric zenith delay and the up component of a positioning solution combine into a single parameter to remove the ill-conditioned problem induced by the correlation of two parameters. This new parameterization coincides with a weighting process of the tropospheric mapping functions and the up components of the design matrix using a scale factor. The main features of the new approach are highlighted, including compatibility, controllability, singularity and redundancy.

INTRODUCTION

The demand for precise and reliable positioning is ever increasing in the industrial as well as in the consumer field. Industrial and commercial activities could be made more cost-effective and even new services could be launched if precise and reliable positioning would be possible for all the needs arising. There are a number of existing and emerging applications which require real-time processing, high data rates (up to a 100 Hz), and high accuracy (better than a few cm) over long-ranges (up to a few 100s of km) with possible high platform dynamics. The most common approach for achieving high performance with GPS technology in such demanding applications is RTK-style processing. For example, RTK technology has been used for machine guidance and control such as gantry crane auto-steering, precision farming and agriculture, robotic lawnmowers, automated ground vehicles and so on. Amongst the requirements of such demanding applications, the ability of long-range RTK has been mainly driven by economic reasons and eventually, turns out to be a major trend in the market.

As an efficient approach to accomplishing long-range RTK, network RTK based on multiple reference stations has been used [Fotopoulos and Cannon, 2001; Wubbena et al., 2001; Landau et al., 2002; Rizos, 2002; Kashani et al., 2004]. The integration of several reference stations into a combined network provides a capability for modeling the error sources at a rover within the network and enables lengthening the baselines up to a few 100s of km.

Despite successful implementation of network RTK for long-range applications, however, its performance is not always comparable to single-baseline RTK operating under short-range situations. As network RTK interpolates error corrections for a rover using the error estimates at reference stations, this approach is vulnerable to localized anomalous errors under unfavourable atmospheric conditions. For example, weather fronts and atmospheric conditions associated with heavy rainfall (but not the rain itself) can cause rapid variations in the tropospheric delay [Gregorius and Blewitt, 1998] and subsequently, the performance of an RTK system can be significantly degraded even across relatively short baselines [Skidmore and Van Graas, 2004; Lawrence et al., 2006]. Also, solar-terrestrial interactions can cause significant changes in the morphology of the ionosphere, changing the propagation delay of GPS signals [Langley, 2000]. During severe ionospheric activity, the correction accuracy deteriorates and adversely affects the ambiguity resolution over the network [Petrovski et al., 2002; Wielgosz et al., 2005].

These localized anomalies in the tropospheric and ionospheric delays are not cancelled in the interpolation procedure used for deriving rover delays. Another challenging situation takes place when a rover is located outside the network boundary. Under such an exceptional situation, network RTK must extrapolate error corrections for the rover to provide seamless RTK solutions. In localizing and extrapolating error corrections, network RTK can face the same challenges as single-baseline RTK.

UNB's Previous Work

Our previous approach for meeting the challenges related with long-range RTK applications was to develop a practical long-range, single-baseline RTK technique which overcomes pitfalls in the conventional single-baseline RTK and complements network RTK, as well. This approach was based on a well proven RTK structure which typically consists of a 3-step procedure: a float ambiguity solution, ambiguity search and validation, and a fixed ambiguity solution. Originally, this structure was built for short-range RTK applications and has satisfied most high performance requirements. In fact, this structure is still feasible for long-range RTK applications if a few add-on features are carefully developed and choreographed. These add-on features include new techniques for handling the tropospheric and ionospheric delays: an adaptive estimator for the tropospheric zenith delay and an ionosphere-nullification technique [Kim and Langley, 2005; 2007a; 2007b]. The main features of our previous approach are highlighted below.

Given L1 and L2 DD (double-differenced between satellites and receivers) carrier-phase observation equations, the unknown parameters can be deliberately separated into three sub-groups, including receiver position and tropospheric delay, ambiguity and ionospheric delay, and satellite orbit error.

Since the effect of satellite navigation message orbit errors is insignificant for baselines up to a few 100s of km and can be virtually eliminated using the International GNSS Service (IGS) ultra-rapid orbit products, it can be safely neglected in real-time applications. Using the well-known "rule of thumb" validated using IGS data, an approximate baseline component error becomes around 1 cm over a baseline of 100 km with around 2 m orbital error [Beutler, 1998; Ziebart et al., 2002].

As is well known, the ionospheric delays can be derived from the geometry-free combination (that is, the difference of L1 and L2 carrier-phase observations in distance units) once the L1 and L2 ambiguity parameters are known. This implies that the ionospheric delays are dependent on the ambiguity parameters and consequently, can be estimated in the ambiguity search process. This is the key idea of the ionosphere-nullification technique (i.e., ionosphere-free ambiguity search process) [Kim and Langley, 2005; 2007a]. Compared with the conventional short-range RTK ambiguity search process, some effort must be extended in building an efficient ambiguity search engine because this technique requires a search engine that simultaneously determines the L1 and L2 ambiguities.

The receiver position and tropospheric delays can be instantaneously estimated at every epoch using least-squares estimation in conjunction with the ionosphere-nullification technique. In this case, the degree of correlation between satellite geometry (connected with the receiver position) and tropospheric mapping functions (connected with the tropospheric zenith delay) turns out to be critical to the performance of the least-squares estimator. Generally, an error in the tropospheric zenith delay is almost indistinguishable from the unmodelled height component at high elevation angles because the two parameters are highly correlated. To break up their correlation, satellites observed at low elevation angles must be included in the observation equations. However, satellites observed at low elevation angles are not always favourable because the GPS signals are more susceptible to the errors (e.g., multipath) and the receiver system noise at low elevation angles.

In case no satellites are available at low elevation angles, an adaptive estimator of the tropospheric zenith delay can be introduced in the observation equations. Since the tropospheric delays will not vary dramatically under a typical atmospheric condition over a short time period, it might be better to estimate adaptively the tropospheric zenith delay. This can be done by introducing a forgetting factor which is the reciprocal of the correlation time (or a smoothing time interval). This adaptive estimator can capture the changes of satellite geometry and mapping functions over a relatively short time period, enabling the tropospheric zenith delay to be distinguished from the height component correction.

PROPOSED APPROACH

As a matter of fact, the residual tropospheric delay is still the most challenging error source for long-range RTK applications. In our previous approach [Kim and Langley, 2007b], the ionosphere-nullification technique does not require any a priori information of the ionospheric delays in resolving the L1 and L2 ambiguities while the prediction values of the residual tropospheric delays are fed into the least-squares estimation. Therefore, incorrect prediction values of the residual tropospheric delays can deteriorate the overall performance of the ambiguity search process and eventually, may result in incorrect positioning solutions. This situation is more likely to occur if no satellite is available at low elevation angles and/or the adaptive estimator of the tropospheric zenith delay fails to track varying atmospheric conditions.

Two approaches have been proposed to obtain more realistic prediction values of the residual tropospheric delays. Using the ionosphere-free linear combination, a sequential least-squares estimator can be implemented as a parallel process to predict the residual tropospheric delays at a given epoch. This estimator has been used in conventional long-range, single-baseline RTK. If the error corrections of the tropospheric delays are available from network RTK, they can be also used as (a priori) prediction values. Using either of the tropospheric prediction values, the proposed approach can be implemented in a back-up process to complement network RTK.

In this paper, we further propose a new approach to overcome the challenges associated with the residual tropospheric delay. This approach combines the residual tropospheric delay and the height component of the positioning solution into a single parameter to remove a singularity problem due to the correlation of the two parameters.

The Observation Model

The DD carrier-phase observations are used in our approach. The linearized GPS carrier-phase observation model for long-range single-baseline applications is given as:

$$\mathbf{y}_i = \mathbf{Hx} + \mathbf{s} + \mathbf{T} - \mathbf{I}_i + \lambda_i \mathbf{N}_i + \mathbf{e}_i, \quad Cov[\mathbf{e}_i] = \mathbf{Q}_{\mathbf{y}i}, \quad i = 1 \text{ or } 2, \tag{1}$$

where $\mathbf{y}$ is the vector of DD carrier-phase observation differences in distance units; $\mathbf{x} = [dn \quad de \quad du]^T$ is the vector of unknown baseline component increments given in local geodetic coordinates (i.e., *dn*-north, *de*-east and *du*-up component); $\mathbf{s}$ is the vector of orbit error contributions to the DD carrier-phase observations; $\mathbf{T}$ is the vector of DD tropospheric delays; $\mathbf{I}$ is the DD first order ionospheric delay parameter vector where $\mathbf{I}_2 = \left(f_{L1}^2 / f_{L2}^2\right)\mathbf{I}_1$; $\mathbf{H}$ is the design matrix corresponding to $\mathbf{x}$; $\mathbf{N}$ is the vector of DD ambiguities; f and λ are the frequency and wavelength of the carrier-phase observations, respectively; $\mathbf{e}$ is the noise vector including multipath, residual ionospheric delay (e.g., higher-order ionospheric effects [Bassiri and Hajj, 1993; Hoque and Jakowski, 2007]) and receiver system noise; $Cov[\cdot]$ represents the variance-covariance operator; $\mathbf{Q}_\mathbf{y}$ is the variance-covariance matrix of the observations; and i indicates the L1 or L2 signal.

By parameterizing the tropospheric delay $\mathbf{T}$ (see Appendix), and ignoring the orbit error term $\mathbf{s}$ in Eq. (1), we will have a new carrier-phase observation model for long-range single-baseline applications as:

$$\mathbf{y}_i' = \mathbf{Hx} + \mathbf{m}_w \tau_{wz} - \mathbf{I}_i + \lambda_i \mathbf{N}_i + \mathbf{e}_i, \quad Cov[\mathbf{e}_i] = \mathbf{Q}_{\mathbf{y}i}, \quad i = 1 \text{ or } 2, \tag{2}$$

where $\mathbf{y}_i' = \mathbf{y}_i - \mathbf{T}_h$; $\mathbf{T}_h$ is the vector of the hydrostatic (or dry) delay; $\mathbf{m}_w$ is the vector of the non-hydrostatic (or wet) mapping functions; and τ_{wz} is the wet zenith delay. It is assumed in Eq. (2) that the hydrostatic delay $\mathbf{T}_h$ can be computed using accurate real-time meteorological data available at a reference station and a rover. In addition, it is assumed that horizontal atmospheric gradients and azimuthal asymmetry are insignificant under typical atmospheric conditions.

Motivations

As mentioned previously, variations in the tropospheric zenith delay are almost indistinguishable from those in the up component at high elevation angles because the two parameters are highly correlated. Figure 1 shows the relationship between the two coefficients – the wet mapping function $\mathbf{m}_w$ and the up component of the design matrix $\mathbf{h}_u$ – associated with the wet zenith delay τ_{wz} and the up component increment du of a positioning solution, respectively. The top and middle panels show the behaviour of two coefficients corresponding to the elevation angles, respectively. The bottom panel shows the relationship of the two coefficients. As illustrated in the example of Figure 1, the two coefficients are almost linearly correlated above a 20 degree elevation angle, which means that τ_{wz} and du will have almost 100% correlation. At a low elevation angle (e.g., lower than 10 degrees), their correlation becomes much weaker.

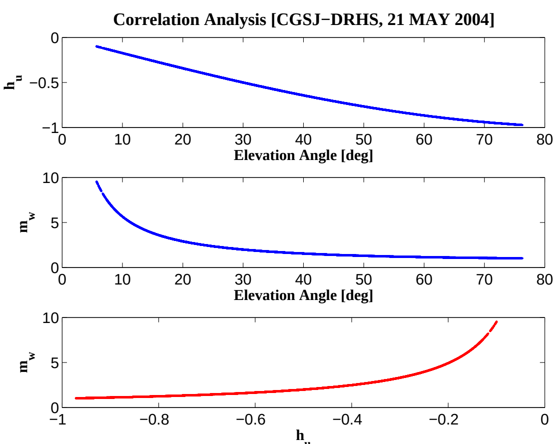

Figure 1. Relationship between the wet mapping function ($\mathbf{m}_w$) and the up component of the design matrix ($\mathbf{h}_u$).

Generally, the performance of the least-squares estimator will deteriorate if the parameters to be estimated are highly correlated. Typically, satellites being observed at low elevation angles can help the least-squares estimator break up the correlation associated with τ_{wz} and du. If no satellite is available at low elevation angles, an adaptive estimator of the tropospheric zenith delay can relieve the problem to some degree.

As far as we know, no one has yet tried another approach to overcome the correlation problem. Since τ_{wz} and du are aligned essentially in the same zenith direction for most stable positioning application (see Figure 2), the two parameters can be combined into another single parameter also aligned with the zenith direction.

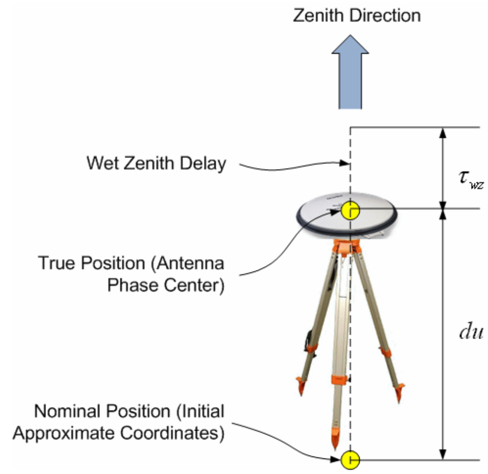

Figure 3. Geometrical relationship between the wet zenith delay and the up component increment of a positioning solution.

New Parameterization

To derive a mathematical expression for the new parameter, we can re-group the unknown parameters. Note that the ionospheric delay **I** and ambiguities **N** are resolved in the ambiguity search process using the ionosphere-nullification technique. Therefore, we leave them out in the equations hereafter.

$$\begin{aligned}
\mathbf{y}_i' &= \mathbf{H}\mathbf{x} + \mathbf{m}_w \tau_{wz} + \cdots, \quad i = 1 \text{ or } 2 \\
&= \begin{bmatrix} \mathbf{h}_n & \mathbf{h}_e & \mathbf{h}_u \end{bmatrix} \begin{bmatrix} dn \\ de \\ du \end{bmatrix} + \mathbf{m}_w \tau_{wz} + \cdots \\
&= \begin{bmatrix} \mathbf{h}_n & \mathbf{h}_e \end{bmatrix} \begin{bmatrix} dn \\ de \end{bmatrix} + \begin{bmatrix} \mathbf{h}_u & \mathbf{m}_w \end{bmatrix} \begin{bmatrix} du \\ \tau_{wz} \end{bmatrix} + \cdots
\end{aligned} \tag{3}$$

The second term of the last line in Eq. (3) can be further expressed as:

$$\mathbf{h}_u du + \mathbf{m}_w \tau_{wz} = \mathbf{h}_\alpha du_\alpha, \tag{4}$$

where $du_\alpha \left(= du + \tau_{wz}\right)$ is the new parameter combining the wet zenith delay and the up component, and $\mathbf{h}_\alpha$ is the vector of new coefficients corresponding to the new parameter, given as:

$$
\begin{aligned}
\mathbf{h}_\alpha &= \mathbf{h}_u \frac{du}{du_\alpha} + \mathbf{m}_w \frac{\tau_{wz}}{du_\alpha} \\
&= \alpha \mathbf{h}_u + (1-\alpha)\mathbf{m}_w
\end{aligned} \tag{5}
$$

and

$$
\alpha = \frac{du}{du_\alpha}. \tag{6}
$$

By substituting Eqs. (4), (5) and (6) into Eq. (3), we will have a new observation equation as:

$$
\mathbf{y}'_i = \begin{bmatrix} \mathbf{h}_n & \mathbf{h}_e & \mathbf{h}_\alpha \end{bmatrix} \begin{bmatrix} dn \\ de \\ du_\alpha \end{bmatrix} + \cdots, \quad i = 1 \text{ or } 2 \tag{7}
$$

Main Features

The new parameterization with respect to the wet zenith delay and the up component coincides with a weighting process of the wet mapping function $\mathbf{m}_w$ and the up component of the design matrix $\mathbf{h}_u$ using a scale factor α. Once α is determined, we can carry out the least-squares estimation using Eq. (7). For a given α, therefore, we can solve du_α in the least-squares estimation, which subsequently provides a backward solution of du and τ_{wz} as:

$$
\begin{aligned}
\alpha &= \frac{du}{du_\alpha} && \rightarrow \quad du = \alpha \cdot du_\alpha \\
du_\alpha &= du + \tau_{wz} && \rightarrow \quad \tau_{wz} = du_\alpha - du
\end{aligned} \tag{8}
$$

A few main features of the new approach are highlighted below. More details are discussed in the section "Test Results".

- *Compatibility*
  The α_{LS} derived by the (original) least-squares estimator in Eq. (2) gives an identical backward solution of du and τ_{wz}.

- *Controllability*
  A given α determines a unique solution of du and τ_{wz}, which enables us to control the estimation process.

- *Singularity*
  Avoiding a direct inverse with respect to $[\mathbf{h}_u \quad \mathbf{m}_w]$ solves the singularity problem of the least-squares estimator.

- *Redundancy*
  Combining du and τ_{wz} into a single parameter increases the degrees-of-freedom of the least-squares estimator.

TEST RESULTS

Two GPS reference stations had been deployed at the Canadian Coast Guard building in Saint John, New Brunswick (CGSJ) and at the Digby Regional High School in Digby, Nova Scotia (DRHS), on either side of the Bay of Fundy, near the terminals of an approximately 74 km marine ferry route (see Figure 4). Two geodetic-grade receivers (NovAtel DL-4 receivers and GPS-600 antennas) had been installed at the reference stations. Also, the same type of receiver had been installed on the ferry – the Princess of Acadia. Surface meteorological equipment had also been collocated with the three receivers. This ferry repeats the same routes between two and four times daily, depending upon the season. The Bay of Fundy is located in a temperate climate region with significant seasonal tropospheric variations (e.g., temperatures between -30°C and +30°C). Data had been collected over the course of one year from the daily ferry runs.

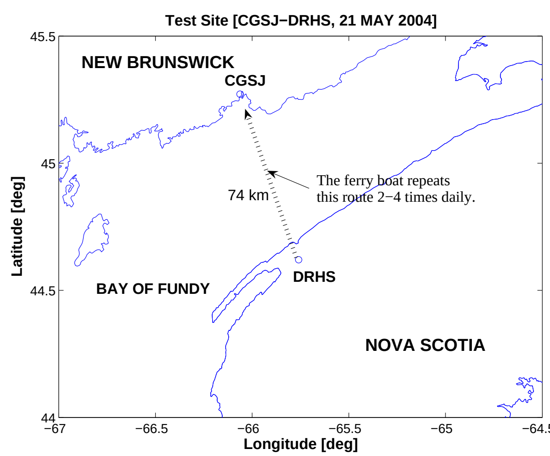

Figure 4. Test site for long-range, single-baseline RTK.

Test Data

To validate the success of our approach, we processed an approximately 1-hour sample of the data recorded at a 1 Hz data rate at the pair of base stations (CGSJ and DRHS) on 21 May 2004. We used a zero degree elevation cutoff angle for data processing. Only static data were processed for this preliminary study. In this case, although test data was recorded in static mode, the data was processed as if it was obtained in kinematic mode. CGSJ was treated as the base station and DRHS as the rover. Figure 5 shows the number of satellites recorded and the elevation angles of the satellites observed.

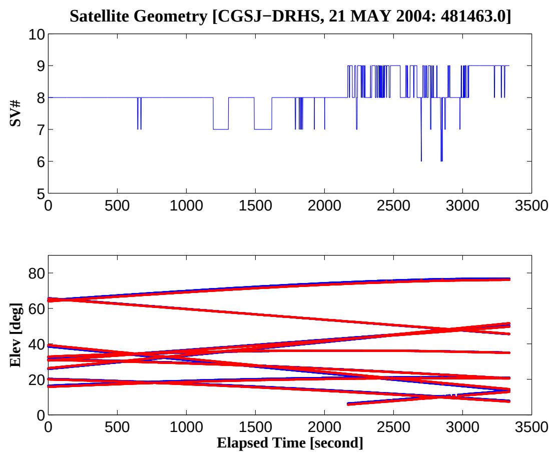

Figure 5. Number of satellites and elevation angles.

Two quality indicators are illustrated in Figure 6. In general, they can be related with the quality information of the parameters being estimated. The top panel shows the dilution of precision (DOP) values (i.e., satellite geometry factors) with respect to the horizontal component (north and east, HDOP), the vertical component (up, VDOP), and the wet zenith delay (τDOP), respectively. The bottom panel shows the correlation coefficients between the up component and the wet zenith delay ($\text{du-}\tau_{wz}$), the north component and the wet zenith delay ($\text{dn-}\tau_{wz}$), and the east component and the wet zenith delay ($\text{de-}\tau_{wz}$).

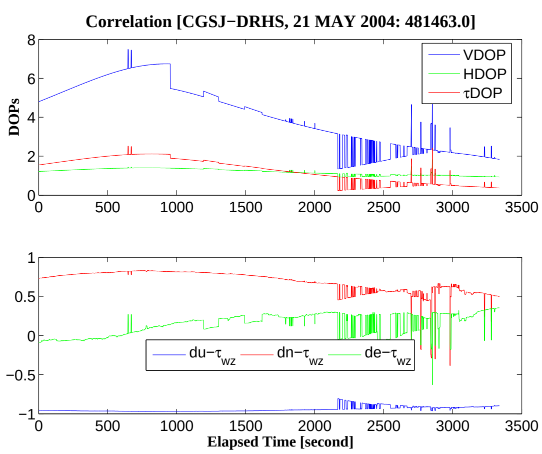

Figure 6. DOP values and correlation coefficients.

As illustrated in Figure 6, the horizontal geometry of the satellites (HDOP) is good over the hour data processing session. On the other hand, the vertical geometry (VDOP) is not good and changing over the period. Therefore, the up component of the positioning solution will be more susceptible to the errors in the observations. As shown in the bottom panel, the correlation between the east position component and the wet zenith delay is weak while the north component is somehow correlated with the wet zenith delay. On the other hand, the correlation between the up component and the wet zenith delay is very strong. Therefore, an error in the tropospheric zenith delay is almost indistinguishable from a change in the up component. Also, an error in the tropospheric zenith delay can be transferred to some degree into the north component.

Previous Approach

The bottom panel in Figure 8 shows the wet zenith delays estimated at every epoch, without the assumption of atmospheric azimuthal asymmetry and use of gradient estimation. Three different types of wet zenith delay estimators are used, including an epoch-by-epoch estimator $\hat{\tau}_k$, an adaptive estimator $\bar{\tau}_k$, and a fixed value $\breve{\tau}_k$. The fixed value of the wet zenith delay, which gave the best positioning solutions (compared with the known coordinates) at $\breve{\tau}_k = 0.028\,\mathrm{m}$, was determined by processing the approximately 1-hour sample of the data recorded at a 1 Hz data rate. These positioning solutions were used as the reference solutions for comparison hereafter. The adaptive estimator was decided by a forgetting factor $\beta\left(=0.001\right)$ which is reciprocal to a smoothing time interval. In this case, the equivalent smoothing time interval was a 1000 seconds $\left(=\left(1/\beta\right)\cdot\left(1/\text{data rate}\right)\right)$. The epoch-by-epoch estimator corresponds to the least-squares estimation of Eq. (2).

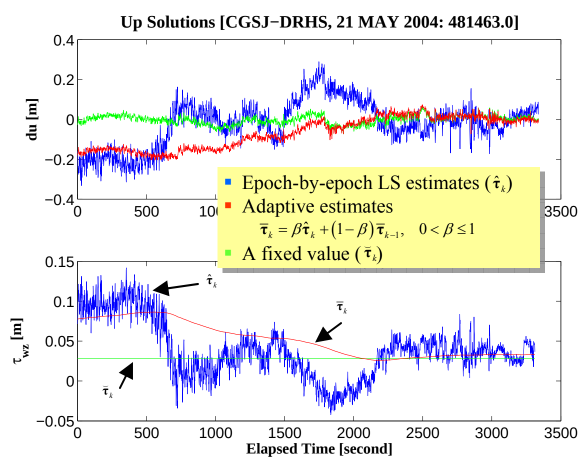

Figure 8. Comparison of the vertical solutions corresponding to the wet zenith delay estimators.

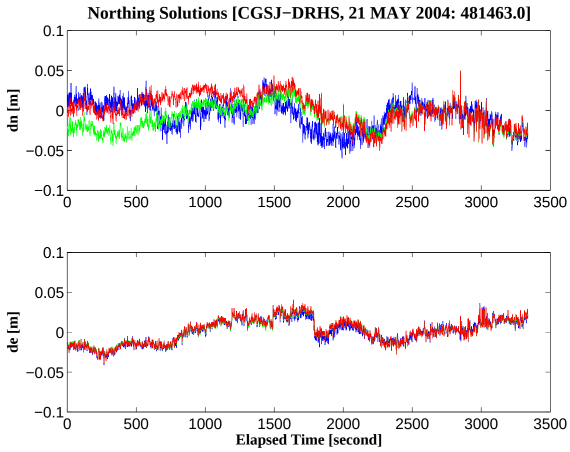

Figure 9. Comparison of the horizontal solutions corresponding to the wet zenith delay estimators.

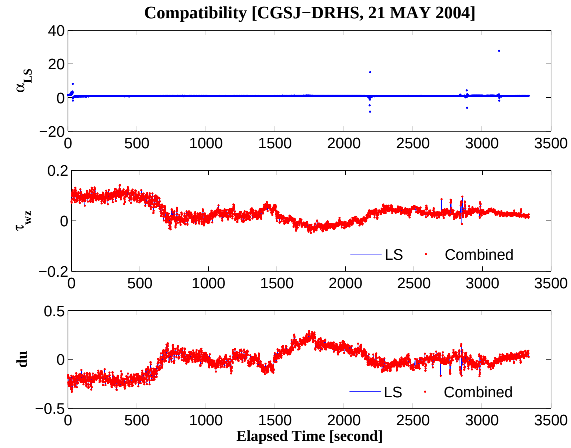

Figure 10. Compatibility of the new approach with the (original) least-squares estimation.

As illustrated in Figure 8, the up solutions show a clear dependency on the wet zenith delay estimators. The up solutions determined by the epoch-by-epoch estimator are noisy and apt to be biased. The adaptive estimator provides less noisy but slowly converging up solutions. On the other hand, the overall difference in the horizontal solutions determined by the wet zenith delay estimators is insignificant as shown in Figure 9. As explained previously, however, the north solutions are affected to some degree by an error in the wet zenith delay.

Compatibility

The up component and the wet zenith delay determined by the (original) least-squares estimation using Eq. (2) are identical to the backward solution in Eq. (9) if the weighting factor α is given as:

$$\alpha_{LS} = \frac{d\hat{u}}{d\hat{u} + \hat{\tau}_{wz}}, \tag{10}$$

where $d\hat{u}$ and $\hat{\tau}_{wz}$ represent the (original) least-squares estimates of the up component and the wet zenith delay, respectively. Figure 10 shows that the new approach is completely equivalent to the (original) least-squares estimation. The compatibility implies that the (original) least-squares estimation is a special case of the proposed approach.

Controllability

The most powerful aspect of the proposed approach is that the estimation process is controllable using α. Figure 11 shows a new α transformed from the original α given by Eq. (10). The vertical (red) line in each panel indicates the α value minimizing the weighted sum of the squared residuals (v^TPv). Various quality measures such as DOP values, correlation coefficients, variances and so on have been used to formulate a transformed α. So far, the solution is more or less based on trial and error. More investigations will be carried out for establishing an optimal procedure in formulating the transformed α in the near future.

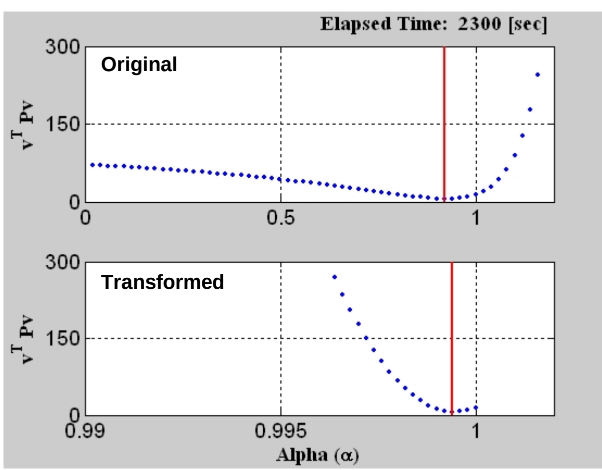

Figure 11. A transformed α controlling the estimation process.

The performance of the proposed approach in terms of controllability is illustrated in Figures 12, 13 and 14. In each figure, the top panel shows positioning solutions estimated by the (original) least-squares estimation using Eq. (2). The middle panel shows the transformed α values.

The bottom panel shows positioning solutions estimated by the new approach using Eq. (7). In both the top and the bottom panels, three different types of wet zenith delay estimators were used, including an epoch-by-epoch estimator $\hat{\tau}_k$ (a blue line), an adaptive estimator $\overline{\tau}_k$ (a red line), and a fixed value $\breve{\tau}_k$ (a green line). Compared with the (original) least-squares estimation, no significant change was found in the horizontal solutions. However, the estimates of the up components were significantly improved when using the proposed approach.

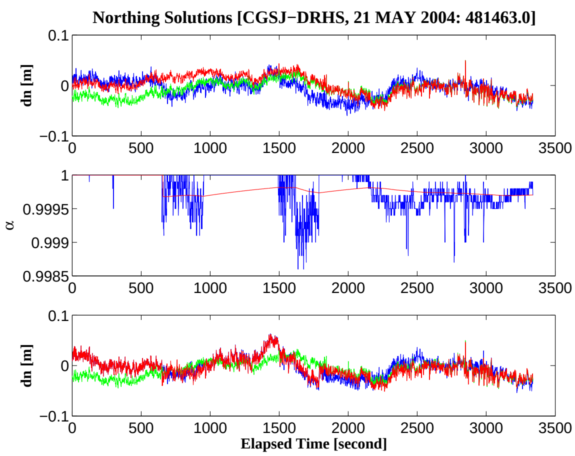

Figure 12. Comparison of the northing solutions.

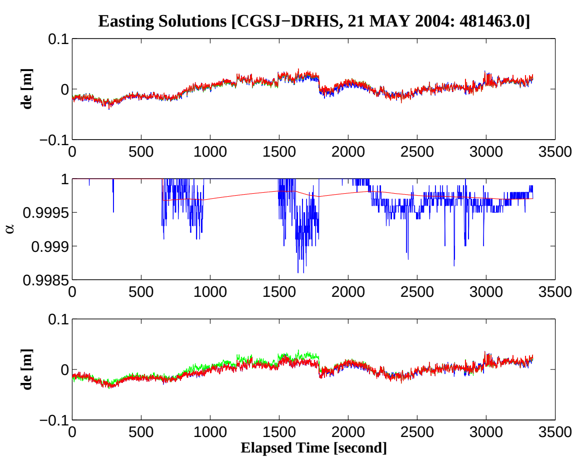

Figure 13. Comparison of the easting solutions.

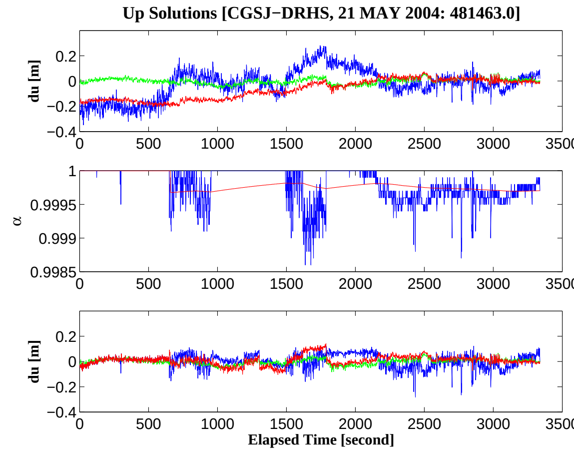

Figure 14. Comparison of the up solutions.

If any unmodelled error in Eq. (2) is unbiased, both approaches will give an identical solution. However, if there is any biased error in the observations, the solution of the (original) least-squares estimation will be biased in the end. On the other hand, the proposed approach is able to de-weight the errors using the transformed α values and eventually, can determine an unbiased solution.

Singularity and Redundancy

By avoiding a direct inverse with respect to $\begin{bmatrix} \mathbf{h}_u & \mathbf{m}_w \end{bmatrix}$ in Eq. (3), the proposed approach solves the singularity problem intrinsic in the (original) least-squares estimation. Also, the new approach combines du and τ_{wz} into a single parameter, which consequently, increases the degrees-of-freedom of the estimation process. To demonstrate these outstanding features, a simulation test was performed. We imposed a 20 degree elevation cutoff angle in processing the original data set. Compared with Figures 5 and 6, this simulation set-up resulted in a poor geometry especially in the vertical direction (see Figure 15). Also, the correlation between the up component and the wet zenith delay in the bottom panel became stronger.

Figures 16 and 17 show the solutions estimated by the (original) least-squares estimation. These solutions are compared with the reference solutions mentioned in the section “Previous Approach”. As illustrated in Figure 16, the simulation did not alter the horizontal solutions significantly. On the other hand, the performance of the (original) least-squares estimation with respect to the up component and the wet zenith delay was very poor (see Figure 17).

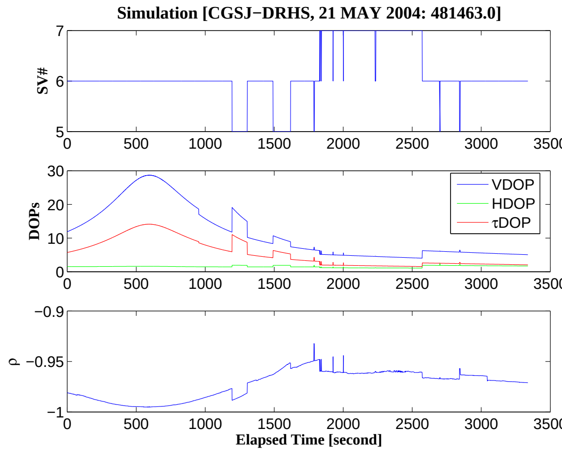

Figure 15. Quality information of the simulation test.

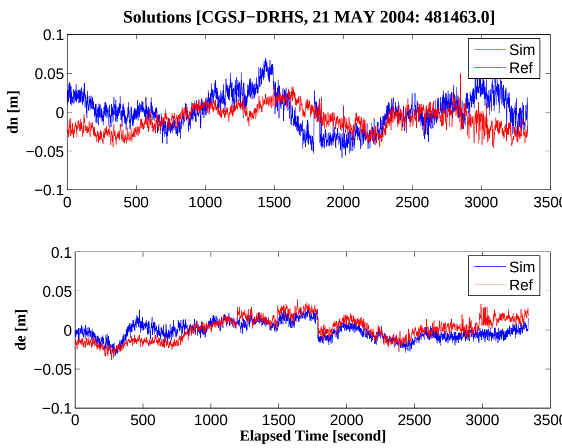

Figure 16. Comparison of the horizontal solution.

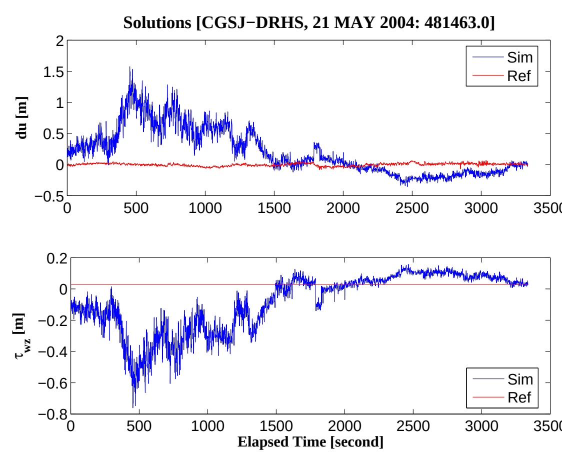

Figure 17. Comparison of the vertical solution and the wet zenith delay.

Figure 18 shows the performance of the proposed approach using the data with a 20 degree elevation cutoff angle. This data mimics a poor geometry scenario. Again, the top panel shows positioning solutions estimated by the (original) least-squares estimation using Eq. (2). The middle panel shows the transformed α values. The bottom panel shows positioning solutions estimated by the new approach using Eq. (7). In both the top and the bottom panels, three different types of wet zenith delay estimators were used. Compared with the (original) least-squares estimation, the new approach improves the up solutions significantly by solving the singularity problem as well as increasing the redundancy of the estimation process.

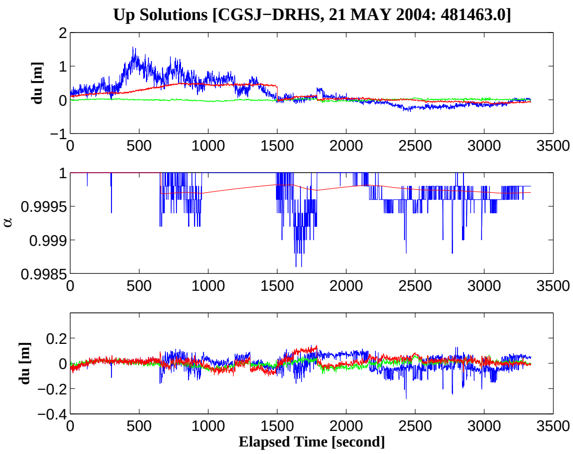

Figure 18. Comparison of the up solutions.

SUMMARY

One of the major challenges in resolving ambiguities for longer baselines is the presence of unmodelled atmospheric (i.e., ionospheric and tropospheric) delays. In our previous work, we proposed the ionosphere-nullification technique which can virtually eliminate the large first-order ionospheric effects using the ionosphere observable in the simultaneous L1 and L2 ambiguity search process. We also proposed the adaptive estimator for estimating the tropospheric delays. Although we have significantly improved the handling of the unmodelled atmospheric delays, we have often found that the residual tropospheric delay is still the most challenging error source for long-range RTK applications.

Theoretically, the two coefficients associated with the tropospheric zenith delay and the up component of a positioning solution – the tropospheric mapping functions and the up components of the design matrix – are almost linearly correlated (i.e., almost 100% correlation) above a 20 degree elevation angle. Therefore, the tropospheric zenith delay is almost indistinguishable from the up component at high elevation angles. If the parameters to be estimated are highly correlated, the performance of the least-squares estimator will deteriorate. In this respect, satellites observed at low elevation angles can help the least-squares estimator break up the correlation associated with the two parameters. If no satellite is available at low elevation angles, an adaptive estimator of the tropospheric zenith delay can relieve the problem to some degree.

In this paper, we proposed a new approach to overcome the challenges associated with the residual tropospheric delay. This approach combines the tropospheric zenith delay and the height component of the positioning solution to remove the singularity problem induced by the correlation of two parameters. Since the two parameters are aligned essentially in the same zenith direction, they can combine into another single parameter pointing at the zenith direction. This new parameterization corresponds to a weighting process of the wet mapping functions and the up components of the design matrix using a scale factor.

We highlighted a few main features of the new approach in this paper. The original least-squares estimation is a special case of the proposed approach (compatibility). The solution of the original least-squares estimation will be biased if there is any biased error in the observations. However, the proposed approach is able to de-weight the errors using a scale factor and eventually, can determine an unbiased solution (controllability). By avoiding a direct inverse with respect to the wet zenith delay and the up component, the proposed approach solves the ill-conditioned problem intrinsic in the original least-squares estimation (singularity). Also, the new approach combines two parameters into a single parameter, which consequently, increases the degrees-of-freedom of the estimation process (redundancy).

Future Work

The most powerful aspect of the proposed approach is that the estimation process is controllable using a scale factor. To formulate a generalized scale factor, we have used various quality measures such as DOP values, correlation coefficients, variances and so on. We have achieved reasonable results based on trials and errors. We plan to investigate further this issue in the near future.

In this paper, the approach was based on typical atmospheric conditions. More specifically, it was assumed that horizontal atmospheric gradients and azimuthal asymmetry are insignificant under typical atmospheric conditions. Further investigation will be carried out to validate if the approach will still work under abnormal conditions.

ACKNOWLEDGEMENTS

The authors would like to thank the U.S. Office of Naval Research for funding some parts of the Bay of Fundy research project during 2003-2004 through an agreement with the University of Southern Mississippi. This project yielded the data used for the work report in this paper. Some of the research was carried out under contract specifically for GNSS simulation system development for modeling environmental errors. The support of the Korea Astronomy and Space Science Institute is gratefully acknowledged.

REFERENCES

Bassiri, S. and G. A. Hajj (1993). “Higher-order ionospheric effects on the global positioning system observables and means of modeling them.” Manuscripta Geodaetica, Vol. 18, pp. 280-289.

Beutler, G. (1998). “GPS satellite orbits.” In GPS for Geodesy, 2nd edition, edited by P. J. G. Teunissen and A. Kleusberg, Chapter 2, pp. 43-110, Spring-Verlag, New York.

Chen, G. and T. A. Herring (1997). “Effects of atmospheric azimuthal asymmetry on the analysis of space geodetic data.” Journal of Geophysical Research, Vol. 102, No. B9, pp. 20489-20502.

Davis, J. L., T. A. Herring, I. I. Shapiro, A. E. E. Rogers, and G. Elgered (1985). “Geodesy by radio interferometry: Effects of atmospheric modelling errors on estimates of baseline length.” Radio Science, Vol. 20, No. 6, pp. 1593-1607.

Fotopoulos, G. and M. E. Cannon (2001). “An overview of multiple-reference station methods for cm-level positioning.” GPS Solutions, Vol. 4, No. 3, January, pp. 1-10.

Gregorius, T. and G. Blewitt (1998). “The effect of weather fronts on GPS measurements.” GPS World, Vol. 9, No. 5, May, pp. 52-60.

Herring, T. A. (1992). “Modeling atmospheric delays in the analysis of space geodetic data.” Proceedings of Refraction of Transatmospheric Signals in Geodesy, Netherlands Geodetic Commission Series, Vol. 36, pp. 157–164.

Hoque, M. M. and N. Jakowski (2007). “Higher order ionospheric effects in precise GNSS positioning.” Journal of Geodesy, Vol. 81, No. 4, 2007, pp. 259-268.

Kashani, I., D. Grejner-Brzezinska and P. Wielgosz (2004). “Towards instantaneous RTK GPS over 100 km distances.” Proceedings of ION 60th Annual Meeting, Dayton, Ohio, 7-9 June, pp. 679-685.

Kim, D. and R. B. Langley (2005). “Nullification of differential ionospheric delay for long-baseline real-time kinematic applications.” Proceedings of ION 61st Annual Meeting, Cambridge, Massachusetts, 27-29 June, pp. 949-960.

Kim, D. and R. B. Langley (2007a). “Ionosphere-nullification technique for long-baseline real-time kinematic applications.” Navigation: Journal of the

Institute of Navigation, Vol. 54, No. 3, Fall, pp. 227-240.
Kim, D. and R. B. Langley (2007b). “Long-range single-baseline RTK for complementing network-based RTK.” Proceedings of ION GNSS 2007, Fort Worth, Texas, 25-28 September, pp. 639-650.
Landau, H., U. Vollath and X. Chen (2002). “Virtual reference station systems.” Journal of Global Positioning Systems, Vol. 1, No. 2, pp. 137-143.
Langely, R. B. (2000). “GPS, the ionosphere, and the solar maximum.” GPS World, Vol. 11, No. 7, July, pp. 44-49.
Lawrence, D., R. B. Langley, D. Kim, F.-C. Chan and B. Pervan (2006). “Decorrelation of troposphere across short baselines.” Proceedings of IEEE/ION PLANS 2006, San Diego, California, 24-27 April, pp. 94-102.
McCarthy, D. D. and G. Petit (2003). “International Earth Rotation and Reference Systems Service Conventions 2003, IERS Technical Note No. 32.” [Online] 7 September 2008. <http://www.iers.org/documents/publications/tn/tn32/tn32.pdf>.
Niell, A. E. (1996). “Global mapping functions for the atmospheric delay at radio wavelengths.” Journal of Geophysical Research, Vol. 101, No. B2, pp. 3227–3246.
Petrovski, I., S. Kawaguchi, H. Torimoto, B. Townsend, S. Hatsumoto and K. Fuji (2002). “An impact of high ionospheric activity on MultiRef RTK network performance in Japan.” Proceedings of ION GPS-2002, Portland, Oregon, 24-27 September, pp. 2247-2255.
Rizos, C. (2002). “Network RTK research and implementation - A geodetic perspective.” Journal of Global Positioning Systems, Vol.1, No.2, pp. 144-150.
Rocken, C., T. Van Hove, J. Johnson, F. Solheim and R. Ware (1995). “GPS/STORM – GPS sensing of atmospheric water vapour for meteorology.” Journal of Atmospheric and Oceanic Technology, Vol. 12, 1995, pp. 468-478.
Saastamoinen, J. (1972). “Atmospheric correction for the troposphere and stratosphere in radio ranging of satellites.” Geophysical Monograph, Vol. 15, pp. 247–251.
Skidmore, T. and F. Van Graas (2004). “An investigation of tropospheric errors on differential GNSS accuracy and integrity.” Proceedings of ION GNSS 2004, Long Beach, California, 21-24 September, pp. 2752-2760.
Wielgosz, P., I. Kashani and D. Grejner-Brzezinska (2005). “Analysis of long-range network RTK during a severe ionospheric storm.” Journal of Geodesy, Vol. 79, No. 9, December, pp. 524-531.
Wubbena, G., A. Bagge and M. Schmitz (2001). “RTK Networks based on Geo++® GNSMART - Concepts, implementation, results.” Proceedings of ION GPS 2001, Salt Lake City, Utah, 11-14 September, pp. 368-378.
Ziebart, M., P. Cross and S. Adhya (2002). “Modeling photon pressure: The key to high-precision GPS satellite orbits.” GPS World, Vol. 13, No. 1, January, pp. 43-50.

APPENDIX

Tropospheric Delays

In precise applications requiring millimetre accuracy, the tropospheric delay can be estimated by a simple parameterization. The line of sight delay D is expressed as a function of four parameters as follows [McCarthy and Petit, 2003]:

$$D = m_h(el)D_{hz} + m_w(el)D_{wz} + m_g(el)\left[G_N\cos(az) + G_E\sin(az)\right] \quad \text{(A1)}$$

where D_{hz} is the zenith hydrostatic delay; D_{wz} is the zenith non-hydrostatic or wet delay; G_N and G_E are the north and east delay gradient in distance units, respectively; m_h , m_w and m_g are the hydrostatic, wet and gradient mapping functions, respectively; el is the non-refracted elevation angle at which the signal is received; and az is the azimuth angle at which the signal is received, measured east of north.

Under typical atmospheric conditions, GPS data may not have the sensitivity to detect atmospheric gradients and azimuthal asymmetry as included in Eq. (A1). In such a case, the tropospheric delay can be estimated by restricting the parameterization to the zenith delay components, such that:

$$D = m_h(el)D_{hz} + m_w(el)D_{wz}\,. \quad \text{(A2)}$$

Hydrostatic Delay For the most accurate a priori hydrostatic delay, the formula of Saastamoinen [1972] as given by Davis et al. [1985] is used in this paper as:

$$D_{hz} = \frac{(0.0022768 \pm 0.0000005)P_0}{1 - 0.00266(\cos 2\phi) - 0.00028H}\,, \quad \text{(A3)}$$

where P_0 is total atmospheric pressure in millibars at the antenna reference point; ϕ is the geodetic latitude of the site; and H is the height above the geoid (km).

Mapping Functions For the hydrostatic and wet mapping functions, Niell’s NMF (New Mapping

Functions) [Niell, 1996] are used in this paper. The NMF adopts the same form of Herring [1992] as:

$$f(el,a,b,c)=\frac{1+\dfrac{a}{1+\dfrac{b}{1+c}}}{\sin(el)+\dfrac{a}{\sin(el)+\dfrac{b}{\sin(el)+c}}}, \tag{A4}$$

In the NMF, unlike the Herring model, the hydrostatic mapping function is dependent on latitude, season (i.e., day of the year) and the height above the geoid of the point of observation while the wet mapping function is dependent on latitude only. The NMF are given by

$$\begin{aligned} m_h(el) &= f_h(el,a,b,c)+\left[\frac{1}{\sin(el)}-f_{ht}(el,a,b,c)\right]H \\ m_w(el) &= f_w(el,a,b,c), \end{aligned} \tag{A5}$$

where again, *el* is the elevation angle at which the signal is received; H is the height above the geoid (km); and subscripts *h*, *w* and *ht* indicate that the function *f* uses the coefficients *a*, *b* and *c* corresponding to the hydrostatic and wet mapping functions and height correction, respectively.

For the gradient mapping function, Chen and Herring [1997] can be used as:

$$\mathrm{m_g}(el)=\frac{1}{\sin(el)\tan(el)+0.0032}. \tag{A6}$$

Estimation Model

Assuming that accurate real-time meteorological data are available at a reference station and a rover, we can use Eq. (A3) to remove the hydrostatic delay in Eq. (A2), without the assumption of atmospheric azimuthal asymmetry and use of gradient estimation. To avoid a mathematical correlation between the partial derivatives of the tropospheric delay at two stations, the levering technique [Rocken et al., 1995] can be used, which fixes the tropospheric delay at the reference station and estimates the relative delay at the rover. Then, from Eq. (A2), the DD tropospheric delay *T* is given by

$$T_{AB}^{uv}=SD_B^{uv}(D)-SD_A^{uv}(D)=T_h+m'_w\tau_{wz}, \tag{A7}$$

where $SD(\cdot)$ is the single-difference (between satellites *u* and *v*) operator; subscripts *A* and *B* indicate a reference station and a rover, respectively; and

$$T_h=SD_B^{uv}(m_hD_{hz})-SD_A^{uv}(m_hD_{hz}) \tag{A8}$$

$$m'_w=m'_{w,B}=SD_B^{uv}(m_w) \tag{A9}$$

$$\tau_{wz}=\tau_{wz,B}-\left(m_w'^T m_w'\right)^{-1}m_w'^T m'_{w,A}\tau_{wz,A}. \tag{A10}$$